International Journal of Computing, SPECAL ISSUE: Intelligent Data Acquisition and Advanced Computing Systems, 7(2):pp.73-83

Mobile Robot Localization using WLAN Signal Strengths

Christof Röhrig, and Frank Künemund

***Abstract*—Many buildings are already equipped with a WLAN infrastructure, as an inexpensive communication technology. In this paper two methods that estimate the position and the heading (pose) of a mobile robot using WLAN technology are described. The proposed techniques for localizing a mobile robot are based on the use of received signal strength values of WLAN access points in range. Both use a radio map based method. For interpolation of the radio map weigthed Euclidean distance and Euclidean distance in combination with Delaunay triangulation is proposed. Measured signal strength values of an omnidirectional antenna and a beam antenna are compared with the values of a radio map, in order to estimate the pose of a mobile robot, whereby the directionality of the beam antenna is used to estimate the heading of the robot. The paper presents the experimental results of measurements in an office building.**

***Index Terms*—Mobile robots, global localization, pose estimation, WLAN, received signal strength.**

I. Introduction

Navigation is a key ability of mobile robots. The task of navigation can be divided into localization and path planning. Aim of localization is to estimate the pose (position and heading) of a mobile robot with respect to its environment. There are three different kinds of localization problems in mobile robotics: position tracking, global localization and kidnapped robot problem. Position tracking requires knowledge of the start position and is also known as local localization. The problem is called global localization, if there is no priori estimate of the pose. The kidnapped robot problem describes a situation, where a localized robot is moved to a different place without its knowledge. It is often used to test a robot's ability to recover from localization failures. Approaches which are capable of solving the global localization problem can be modified such that they can also solve the kidnapped robot problem [1].

Usually robot odometric sensors are used to solve the localization problem of wheeled robots. Odometric sensors provide information about robot movements, but the provided information is noisy and accumulates errors over time. Odometrie is accurate enough for local movements but is not suitable for long term localization and global localization [2].

Additional sensors such as laser and vision provide information about the environment of a mobile robot. Several methods have been proposed to use this information to estimate the pose of a mobile robot. Unfortunately laser sensors are expensive and vision needs computational overhead of image processing. Furthermore this techniques require a map and usually a start position. If the start position is unknown, the pose have to be searched in the whole map, which is difficult and time consuming in a large environment. A global pose estimation using WLAN technology can support such methods by finding the starting pose. Furthermore it can solve the kidnapped robot problem by detecting localization failures and by providing a new starting pose.

Nowadays mobile robots often are equipped with IEEE 802.11 WLAN adapters, in order to communicate with computers or other mobile devices. Furthermore, many buildings are already equipped with an IEEE 802.11 WLAN infrastructure, as a popular and inexpensive technology. Most WLAN adapters are able to measure the signal strengths of received packets as part of their standard operation. The signal strengths of received packets vary noticeably by changing the position. Thus, the signal strength can be used to estimate the position of a mobile device by cheap technology.

In this paper, the problem of global localization is solved using the WLAN infrastructure in an indoor scenario. It extends the existing WLAN localization techniques in two ways. First, it describes two techniques for estimating the heading of a mobile robot. A measured set of signal strength values of an omnidirectional antenna and a beam antenna is compared with a radio map in order to estimate position and heading of a mobile robot. Second, interpolation is proposed in order to reduce the density of the calibration points in the radio map and thus minimizing the manual effort to build the map. Furthermore the proposed techniques can support other map based pose estimation methods by finding a global start position. The paper extends the work presented in [3] by refining the algorithm of heading estimation and by presenting more experimental results, which show the effectiveness of the technique.

II. Related Work

Up to now there are developed several kinds of localization techniques for the use in wireless networks. A review of the existing techniques is given in [4]. This techniques can be classified by the information they use:

- Connectivity information,
- Angle of Arrival (AoA),
- Time of Arrival (ToA),
- Time Difference of Arrival (TDoA),
- Received Signal Strength (RSS).

Connectivity information is available in all kinds of wireless networks. The accuracy of the localization depends on the range of the used technology and the density of the beacons. In cellular networks, Cell-ID is a simple localization method based on cell sector information [5]. In infrastructure mode of a Wireless LAN (WLAN), the access point (AP) to which the mobile device is currently connected, can be determined since mobile devices know the MAC hardware address of

This work was supported in part by the research program of the University of Applied Sciences Dortmund.

The authors are with the University of Applied Sciences Dortmund, Emil-Figge-Str. 42, 44227 Dortmund, Germany, roehrig@ieee.org

the AP, which they are connected to. Bluetooth is another technology, which allows a relatively accurate localization because of its low radio range [6]. Besides the deployment of Radio Frequency Identification (RFID) in Supply Chain Management [7], the RFID technology is also suitable for position estimation. RFID tags can be deployed at known positions in the environment, in order to obtain position information when they are in range. This information can be be fused with data from other sensors (e.g. odometers) for the purpose of improving the accuracy of localization (see [8] and [9]).

AoA determines the position with the angle of arrival from fixed anchor nodes using triangulation. A method, where a wireless sensor node localizes itself by measuring the angle to three or more beacon signals is in [10] proposed. Each signal consists of a continuous narrow directional beam, that rotates with a constant angular speed. Drawback of AoA based methods is the need for a special and expensive antenna configuration e.g. antenna arrays or rotating beam antennas.

ToA and TDoA estimate the range to a sender by measuring the signal propagation delay. The Cricket localization system [11] developed at MIT utilizes a radio signal and a ultrasound signal for position estimation based on trilateration. TDoA of these two signals are measured in order to estimate the distance between two nodes. This technique can be used to track the position of a mobile robot [12]. ToA as wells as TDoA require a complex wireless network infrastructure, which is usually not present in today's WLAN installations.

RSS information can be used in most wireless technologies, since mobile devices are able to monitor the RSS as part of their standard operation. The distance between sender and receiver can be obtained with the Log Distance Path Loss Model described in [13]. Unfortunately, the propagation model is sensitive to disturbances such as reflection, diffraction and multi-path effects. The signal propagation depends on building dimensions, obstructions, partitioning materials and surrounding moving objects. Own measurements show, that this disturbances make the use of a propagation model for accurate localization in an indoor environment almost impossible [3]. Fingerprinting, which is a method to overcome this disadvantage by utilizing a radio map is in [14] introduced. Fingerprinting is divided in two phases: In the initial calibration phase, the radio map is built by moving around and storing RSS values at various predefined points of the environment. In the localization phase, the mobile device moves in the same environment and the position is estimated by comparing the current RSS values with the radio map. A metric to compare the measured RSS values with the radio map is Euclidean distance proposed by [14]. A Bayesian algorithm is used in [15] and [16] proposed Delaunay triangulation with lines of constant signal strength.

Several methods for localization in WLAN environments using RSS have been developed, in order to improve the accuracy of the estimation. A Kalman filter is proposed by [17], a Monte-Carlo algorithm is used by [18] as well by [19], Statistical learning is applied by [20] and Fuzzy is used by [21] and by [22]. All of these methods utilize a radio map and estimate only the position but not the heading of the mobile device. The main disadvantage of radio map based methods is the high manual effort to build the map in the calibration phase. The use of Delaunay triangulation and interpolation allows a radio map with a low density of calibration points and reduces the time for manual generation of the map [3].

III. Characteristic of Received Signal Strength (RSS)

A. Measurement of Signal Strengths

Most mobile devices are able to monitor the RSS values from APs in range as part of their standard operation. There are two kinds of scanning modes: passive scanning and active scanning. In passive scanning mode the WLAN card is put into monitoring mode and waits for incoming packets. In active scanning mode the mobile device sends a probe request packet on every frequency and waits for the probe response packets of the APs in range. Active scanning is an important feature in WLAN positioning, because it obtains new RSS values of all APs in range at the time of scanning.

B. Modeling of Signal Strength

The propagation model of RSS depends on the free space loss of the signal. The free space loss F is defined as

$$F = \frac{P_{\mathrm{Rx}}}{P_{\mathrm{Tx}}} = \left(\frac{c}{4\,\pi\,d\,f}\right)^2 = \left(\frac{\lambda}{4\,\pi\,d}\right)^2 \tag{1}$$

where P_{Rx} is the power of the received signal, P_{Tx} is the power of the transmitted signal, c is the speed of light, f is the frequency of the signal, d is the distance to the sender and λ is the wavelength of the signal. Equation (1) can be expressed in logarithmic scale:

$$\begin{aligned} F/\mathrm{dB} &= 10\,\log_{10}\left(\frac{P_{\mathrm{Rx}}}{P_{\mathrm{Tx}}}\right) \\ &= -32.4 - 20\,\log_{10}(f/\mathrm{MHz}) - 20\,\log_{10}(d/\mathrm{km}) \end{aligned} \tag{2}$$

where the unit of f is MHz and the unit of d is km.

In an indoor environment, where multi path effects occur, equation (2) leads to the log distance path loss model [13],

$$P_{\mathrm{Rx}}/\mathrm{dBm} = P_0/\mathrm{dBm} - 10\,\gamma\,\log_{10}\left(\frac{d}{d_0}\right) \tag{3}$$

where P_0 is the RSS value at the distance d_0 and γ is the path loss exponent. Parameters P_0, d_0 and γ have to be adapted to the geometry of every room in the building. Fig. 1 compares the log distance model with measurements in an office building. It shows, that there are several measurements with equal signal strength at points with distances of more than 10 m.

The propagation model is sensitive to disturbances as reflections, diffractions and multi-path effects. The signal propagation depends on building dimensions, obstructions, partitioning materials and surrounding moving objects. This problem makes the use of a propagation model for accurate localization in an indoor environment almost impossible.

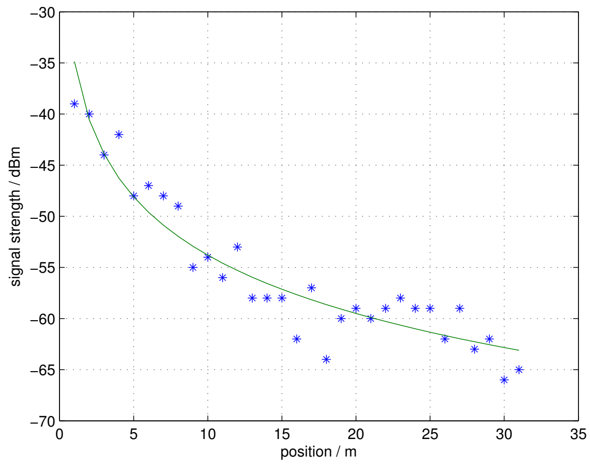

Fig. 1. Propagation model versus real measurements

C. Distribution of Signal Strengths

At a fixed location, the RSS value from an AP varies with time. This effect is caused by people moving around, doors open and closes and other disturbances as Bluetooth senders. Furthermore the distribution of the RSS values are non-Gaussian and the median is not stable over long time. This limits the accuracy of the position estimation significantly. Fig. 2 shows the distributions of measurements at three days at the same location.

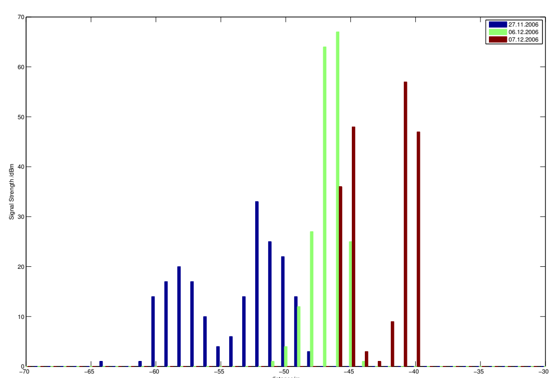

Fig. 2. Distributions of three different measurements

IV. Localization approach

The proposed methods for localizing the mobile robot are based on the use of RSS values of WLAN APs in range. For both, a radio map based method and Euclidean distance in combination with interpolation is used, because of the described reasons. A measured set of RSS values of the omnidirectional antenna and the beam antenna is compared with the radio map. The radio map is built in an initial calibration phase and contains measured sets of RSS values at various predefined poses (x, y, θ). In the experiments, four headings (0°, 90°, 180°, 270°) at every position are stored. In the localization phase, RSS values of several APs are recorded and compared with the radio map. One observation in both phases consists of RSS values of both antennas and all APs. Values of APs out of range are set to a minimal value $c_{\min} = -100\,\text{dBm}$.

A. Estimation of the Position with Euclidean distance

The Euclidean distance is a metric to compare the observations of the localization phase with the radio map. The Euclidean distance between two points $P = (p_1, p_2, \ldots, p_n)$ and $Q = (q_1, q_2, \ldots, q_n)$, is defined as:

$$d = \sqrt{(p_1 - q_1)^2 + (p_2 - q_2)^2 + \cdots + (p_n - q_n)^2} = \sqrt{\sum_{i=1}^{n} (p_i - q_i)^2} \tag{4}$$

In WLAN localization the calibration data are compared with the measured data:

$$d_{j,k} = \sqrt{\sum_{i=1}^{n} \left(c_j^{\text{AP}_i} - s_k^{\text{AP}_i}\right)^2} \tag{5}$$

where $c_j^{\text{AP}_i}$ is the RSS value of AP_i at pose j in the radio map, $s_k^{\text{AP}_i}$ is the RSS value of AP_i at measurement k and n is the total number of APs. The Euclidean distance $d_{j,k}$ is a metric for the distance between the calibration data $c_j^{\text{AP}_i}$ and the measured data $s_k^{\text{AP}_i}$. After calculating $d_{j,k}$ for all calibration points, there will be at least one pose with minimal $d_{j,k}$. One approach is to declare this pose to be the estimated pose of the mobile robot. The accuracy of this method depends beside other factors on the density of the underlying grid of calibration points.

The main problem of radio map based localization systems is the manual generation of the map [23]. In order to reduce the manual effort to build the map, the density of calibration points should be as low as possible [16]. Thus, the interpolation of the estimated position is proposed. In this case a lower density of calibration points is possible. The algorithm that is described in this section interpolates the position and heading of the mobile robot with weighted Euclidean distance. The set of poses $(x_i,\ y_i,\ \theta_i)$ in the database is arranged by the Euclidean distance. A fixed number of poses with least Euclidean distance are used for estimation of the pose.

For interpolation purposes of the position, only the signals of the omnidirectional antenna are used. The weights are built with the reciprocal of the Euclidean distance:

$$\hat{x}_k = \frac{\sum_{j=1}^{J} w_{j,k} \cdot x_j}{\sum_{j=1}^{J} w_{j,k}} \quad \text{with} \quad w_{j,k} = \frac{1}{d_{j,k}}, \tag{6}$$

$$\hat{y}_k = \frac{\sum_{j=1}^{J} w_{j,k} \cdot y_j}{\sum_{j=1}^{J} w_{j,k}}, \tag{7}$$

where J is the number of weighted poses (least Euclidean distance) and $(\hat{x}_k, \hat{y}_k)$ is the estimated position of the mobile robot.

B. Estimation of the heading with Euclidean distance

The estimated heading $(\hat{\theta}_k)$ is interpolated with values of the beam antenna. The headings are weighted and interpolated as vectors:

$$\hat{\theta}_k = \operatorname{atan2}\left(\sum_{j=1}^{J} w_{j,k} \sin\theta_j, \sum_{j=1}^{J} w_{j,k} \cos\theta_j\right), \qquad (8)$$

where atan2() is used in order to interpolate the heading in the range from $-\pi$ to π. Interpolation of the estimated heading allows a relatively low density of headings in the calibration phase. At every location, only four headings ($\Delta 90°$) are stored in the database.

C. Estimation of the position with Delaunay triangulation

This method uses the interpolation based on Delaunay triangulation and lines of constant signal strength (isolines). For interpolation purposes of the position, the received signals of the omnidirectional antenna are used only. With Delaunay triangulation a network of triangles for a set of points (nodes) in the plane is developed, such that no point is inside the circumcircle of any triangle [24]. The nodes are represented by the calibration points. Given a measured RSS value of one AP, triangles whose nodes show RSS values higher and lower than the measured value can be selected. Linear interpolation between node values within the triangle delivers a more detailed radio map consisting of a surface of interpolated RSS values over the triangle. Moreover, it is possible to calculate an interpolated line of constant RSS (isoline) within the triangle and in the whole area of triangulation. Fig. 3 shows the isolines of AP_1, Fig. 4 shows the isolines of AP_2.

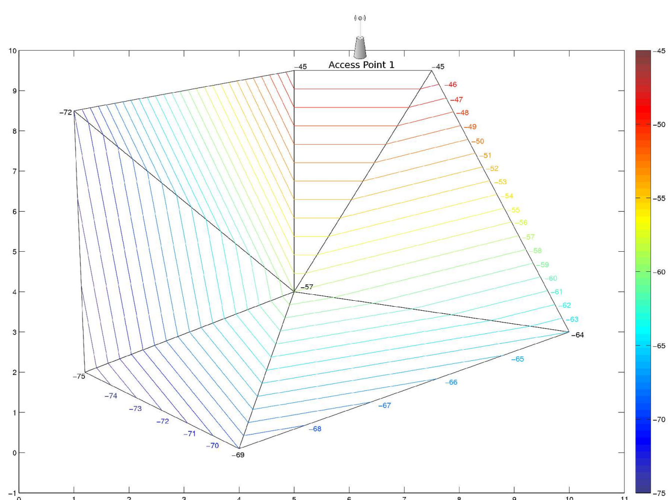

Fig. 3. Lines of constant RSS (isolines) for AP_1

Given two RSS values of different APs, it is possible to select triangles whose interpolation surfaces include the according isolines. If there is an intersection of both isolines, the intersection point within the triangle can be calculated. Fig. 5 shows the merged radio map for AP_1 and AP_2. There are two points of intersection in the radio map for this measurement.

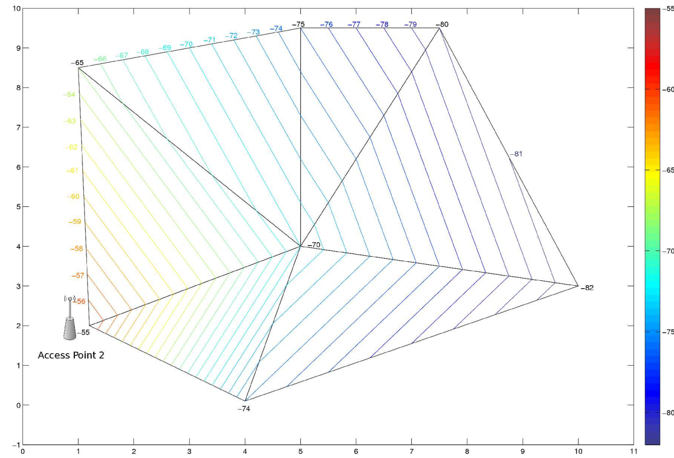

Fig. 4. Lines of constant RSS (isolines) for AP_2

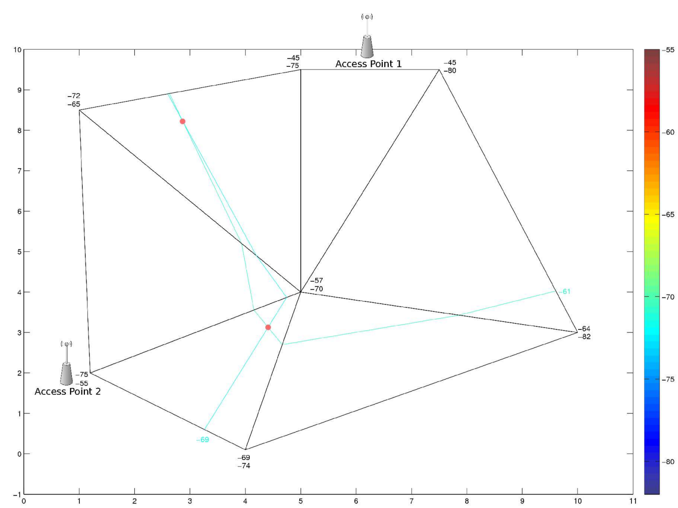

Fig. 5. Merged radio map for AP_1 and AP_2

The pose is estimated using the points of intersection. Points with a large distance to the real position have to be eliminated from the calculation of the estimated position. The elimination of points of intersection is performed using an acceptance circle. This circle is built by a triangle of three points in the radio map with least Euclidean distance to the measured RSS values. It is assumed that the real position is near by this triangle. The center of the circle is the balance point of the triangle. The radius of the circle is built by the largest edge of the triangle. All intersection points outside of the acceptance circle were excluded from the calculation.

Fig. 6 shows a radio map with calibration poses (red arrows), acceptance circle (cyan) and points of intersection (magenta). The real pose of the robot is shown as blue arrow, while the green arrow represents the estimated pose.

The estimated position $(\hat{x}, \hat{y})$ is calculated with weighted

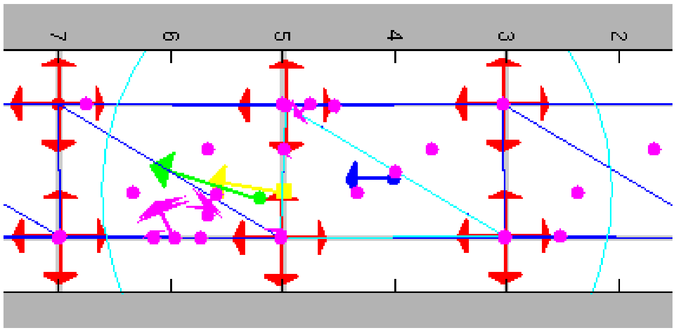

Fig. 6. Visualization of estimation technique

points of intersection:

$$\hat{x} = \frac{\sum_{i=1}^{N} w_i x_i}{\sum_{i=1}^{N} w_i}, \qquad \hat{y} = \frac{\sum_{i=1}^{N} w_i y_i}{\sum_{i=1}^{N} w_i}, \tag{9}$$

where w_i is the weight of intersection x_i, y_i and N is the total number of intersections inside the acceptance circle.

Experiments have shown, that measured RSS values closer to APs are more reliable than those in larger distance [3]. Hence, the weight w_i of intersection i is calculated with RSS values of the crossing isolines:

$$w_i = (s_{i,1} - s_{\min})^2 + (s_{i,2} - s_{\min})^2 \quad \text{with} \quad s_{\min} = -100\,\text{dBm} \tag{10}$$

where $s_{i,1}$ and $s_{i,2}$ are the RSS values of the isolines at intersection i and $s_{\min}$ is the lowest possible RSS value. Higher RSS values are measured closer to APs and lead to larger weights.

D. Estimation of the heading with Delaunay triangulation

Here the heading is estimated with RSS values of the beam antenna. For every point of intersection i a heading $\hat{\theta}_i$ with assigned vector length $\hat{\rho}_i$ is calculated. $\hat{\rho}_i$ is a metric for the quality of the estimation and is used as weight. The estimation of $(\hat{\theta}_i, \hat{\rho}_i)$ is calculated with radio map values of the surrounding triangle:

$$\hat{\theta}_i = \operatorname{atan2}\left(\sum_{j=1}^{J} \frac{w_i}{d_j} \sin\theta_j, \sum_{j=1}^{J} \frac{w_i}{d_j} \cos\theta_j \right), \tag{11}$$

$$\hat{\rho}_i = \sqrt{\left(\sum_{j=1}^{J} \frac{w_i}{d_j} \sin\theta_j \right)^2 + \left(\sum_{j=1}^{J} \frac{w_i}{d_j} \cos\theta_j \right)^2}, \tag{12}$$

where J is the number of weighted headings (with least Euclidean distance) at the nodes of the surrounding triangle, d_j is the Euclidean distance between measured RSS values from the beam antenna and stored RSS values in the radio map and w_i is the weight of intersection i (Eqn. 10). In Fig. 6 $(\hat{\theta}_i, \hat{\rho}_i)$ are represented by magenta arrows.

The heading of the mobile robot $\hat{\theta}$ is estimated by adding the headings of all intersections:

$$\hat{\theta} = \operatorname{atan2}\left(\sum_{i=1}^{N} \sum_{j=1}^{J} \frac{w_i}{d_j} \sin\theta_j, \sum_{i=1}^{N} \sum_{j=1}^{J} \frac{w_i}{d_j} \cos\theta_j \right), \tag{13}$$

$$\hat{\rho} = \sqrt{\left(\sum_{i=1}^{N} \sum_{j=1}^{J} \frac{w_i}{d_j} \sin\theta_j \right)^2 + \left(\sum_{i=1}^{N} \sum_{j=1}^{J} \frac{w_i}{d_j} \cos\theta_j \right)^2}. \tag{14}$$

In Fig. 6 $(\hat{\theta}, \hat{\rho})$ is represented by the green arrow.

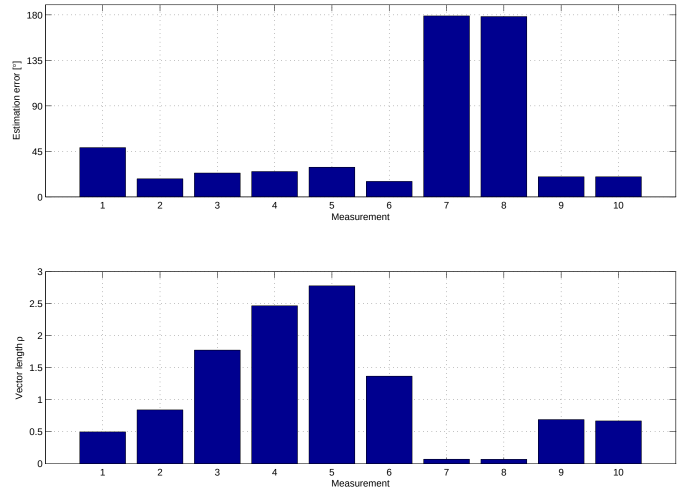

Fig. 7. $\hat{\rho}$ versus estimation error

Fig. 7 compares $\hat{\rho}$ with the estimation error of the heading of 10 measurements at the same location. Measurements 7 and 8 achieve large estimation errors of 180°. This large errors correspond with very low values of $\hat{\rho}$, which indicate a low estimation accuracy. It is proposed to use $\hat{\rho}$ in a later signal processing stage to weight the estimated heading.

V. Experimental Setup

The experiments are carried out with a mobile robot Pioneer3-AT manufactured by ActivMedia (Fig. 8). The robots

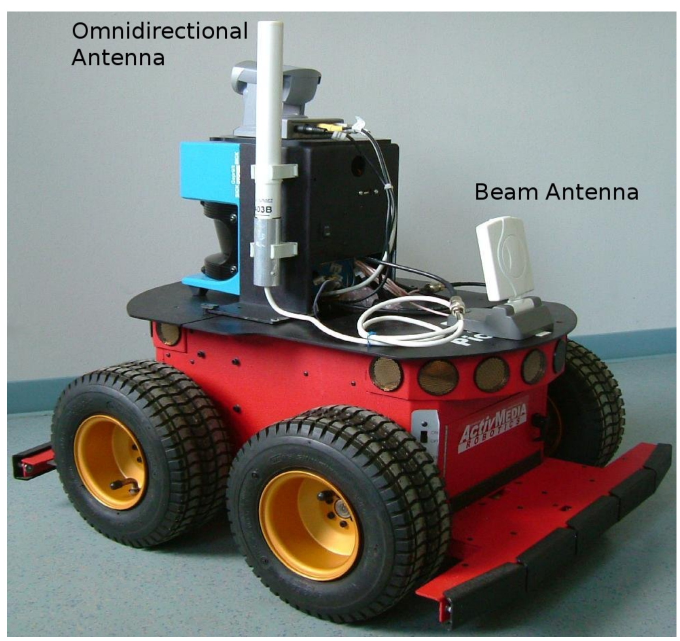

Fig. 8. Pioneer3-AT

is equipped with four wheels which are driven by two motors. This driving concept is called skid-steering locomotion and is similar to the operation of an army tank. Fig. 9 shows the

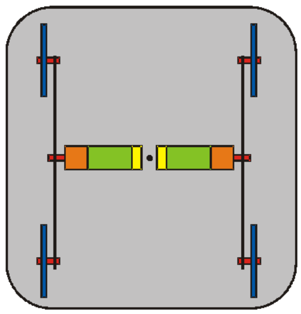

Fig. 9. Skid-steering locomotion

chassis of the robot with four wheels (blue). The wheels are driven over belts and gears (brown) by two motors (green). The position of the mobile robot is estimated with dead reckoning (odometry) over two encoders (yellow), which are mounted at the end of the motors. Position estimation with dead reckoning is highly inaccurate for skid-steered robots, because of slippage, which occurs when the robot moves curves [25]. For global localization, it is necessary to use additional sensor information, as GPS, laser or WLAN RSS.

The robot has four wheels with Since only two motors drive the robot, the wheel speeds on every side of the robot are always the same. This leads to skid-steering kinematics, where the velocities in the robot's local reference frame are given by:

$$\boldsymbol{v}_{\mathrm{R}} = \begin{pmatrix} v_{\mathrm{x}} \\ v_{\mathrm{y}} \\ \omega_{\mathrm{R}} \end{pmatrix} = \begin{pmatrix} \frac{r\cdot\dot{\varphi}_{\mathrm{right}}}{2} + \frac{r\cdot\dot{\varphi}_{\mathrm{left}}}{2} \\ 0 \\ \frac{r\cdot\dot{\varphi}_{\mathrm{right}}}{2b} + \frac{-r\cdot\dot{\varphi}_{\mathrm{left}}}{2b} \end{pmatrix}, \qquad (15)$$

where v_{x} is the velocity in forward direction, v_{y} is the velocity in sidewards direction, ω_{R} is the rotation speed, $\dot{\varphi}_{\mathrm{right}}$ are the angular velocities of the wheels on the right side and $\dot{\varphi}_{\mathrm{left}}$ are the angular velocities of the left side of the robot, r is the radius of the wheels and b is the wheel offset (Fig. 10). The

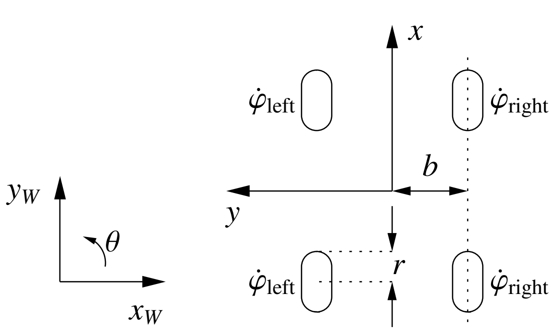

Fig. 10. Velocities in the robot reference frame

velocities in the global reference frame (world frame) depend on the heading (θ) of the robot:

$$\boldsymbol{v}_{\mathrm{W}} = \begin{pmatrix} v_{\mathrm{x}}^{\mathrm{W}} \\ v_{\mathrm{y}}^{\mathrm{W}} \\ \omega_{\mathrm{R}}^{\mathrm{W}} \end{pmatrix} = \begin{pmatrix} \cos\theta & -\sin\theta & 0 \\ \sin\theta & \cos\theta & 0 \\ 0 & 0 & 1 \end{pmatrix} \cdot \begin{pmatrix} v_{\mathrm{x}} \\ v_{\mathrm{y}} \\ \omega_{\mathrm{R}} \end{pmatrix}, \qquad (16)$$

The robot is equipped with an embedded computer for real time robot control and an additional PC with two WLAN cards for communication and localization. One WLAN card is connected to an omnidirectional antenna, the other card is connected to a beam antenna. The directionality of the beam antenna is used to estimate the heading of the robot. Fig. 11 shows the measured polar plots of the beam and the omnidirectional antenna.

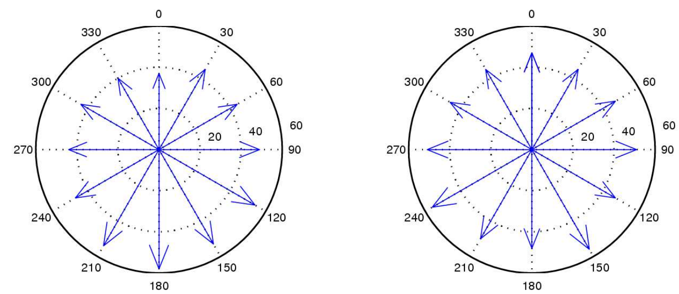

Fig. 11. Characteristic of beam (left) and omnidirectional antenna (right)

A robot server is included in the operating system of the embedded computer. It manages the low-level tasks of robot control and operation, including motion and odometry. The robot server receives the commands from the PC via RS-232 serial link. It is the job of a program running on the PC to perform robotics tasks such as sensor fusion, localization, mapping, and navigation. For programming purposes ActivMedia provides the toolkit ARIA (ActivMedia Robotics Interface for Application) [26]. ARIA is a object oriented, cross-platform (Windows/Linux) toolkit for ActivMedia mobile robots. It is written entirely in C++, but access to the API is also available from the Java programming languages via "wrapper" libraries. ARIA provides an interface to control the robot's velocity, heading, relative heading, and provide detailed information about odometry and operating conditions from the mobile robot.

The operation system on the PC is Ubuntu Linux, which offers support for wireless communication by the wireless extension (WE) [27]. WE is an application programming interface (API) allowing a user space program to configure a WLAN driver and receive statistic information. The WE provide an interface via `ioctl()`, which is documented in `wireless.h`. Good examples for programming WE are the wireless tools for Linux. The program `iwlist` scans the WLAN for accessible APs and monitors the RSS values along with hardware MAC addresses of APs in range. There are two kinds of scanning modes: passive scanning and active scanning. In passive scanning mode the WLAN card is put into monitoring mode and waits for incoming packets. In active scanning mode the mobile device sends a probe request packet on every frequency and waits for the probe response packets of the APs in range. Active scanning is an important feature in WLAN positioning, because the time of the measurements for all RSS values can be determined. Active scanning obtains new RSS values of all APs in range at the time of scanning. Since version 21 of the WE, active scanning mode is supported. In older Linux kernel versions active scanning is not supported and it is necessary to modify the kernel driver in order to receive packets from all APs in range [28]. On up to date Linux distributions, there is no need to modify kernel drivers.

VI. Software Design

The software is divided into three parts: a localization engine, a graphical user interface (GUI) and a WLAN scanner (Fig. 12). The localization engine and the GUI are written in the Matlab script language, the WLAN scanner is implemented in C. The WLAN scanner uses the WE `ioctl()`-Interface for reading RSS values from both WLAN adapters.

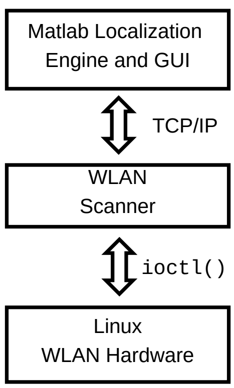

Fig. 12. Design of the localization software

The communication between localization engine and WLAN scanner is build with TCP/IP sockets. Since the localization engine are built on Matlab, it is possible to run it on every computer which offers a Matlab environment and a network access. The GUI is used for monitoring information to the user and for building the radio map. Fig. 13 shows the GUI with a map of a room in the Computer Science building. The red arrows around the red dots show the four headings of the robot in every calibration point of the radio map. The colored lines represent the RSS isolines. In order to build the radio map, the user moves the robot to the predefined poses (red arrows) and stores the RSS values. It is optional to change the Server IP address, the network interfaces for both antennas and the ESSID of the APs. In the localization phase, the blue arrow represents the real pose of the mobile robot and green and yellow arrow visualizes estimated poses. The estimates changes with time without moving the robot, because of the noisy RSS values.

VII. Experimental Results

Experiments are performed in an office building of the Computer Science Department. A test series was measured at the hallway shown in Fig. 6. The existing WLAN-infrastructure was used for the measurements. Fig. 14 shows a histogram of position errors achieved in this test series, which are in a range from 0 to 4 m. In most cases, the accuracy is better than 1.0 m. The accuracy depends directly on the position of the APs in range. For a good and reliable estimation, three ore more APs in a short distance are required. The placement of additional APs increases the accuracy of the estimation.

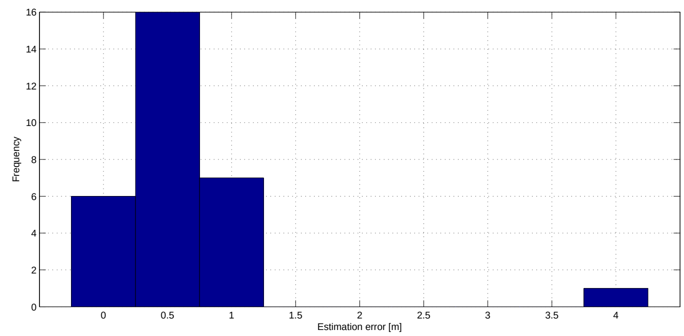

Fig. 14. Histogram of estimation error of position

Fig. 15 compares the estimation accuracy of Delaunay isoline interpolation with Euclidean distance interpolation. In most cases estimations with isoline method achieve a better accuracy than estimations with Euclidean distance only.

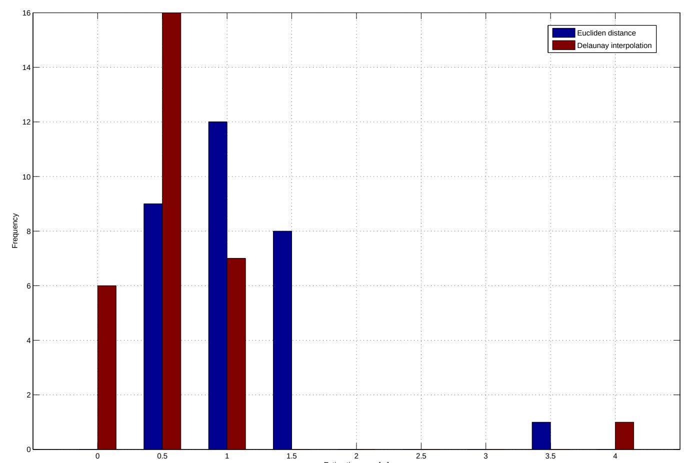

Fig. 15. Comparison of Euclidean distance and Delaunay interpolation

Fig. 16 shows a histogram of the heading error. Heading errors are in the full range from 0 to 180°. In most cases an accuracy better than 45° can be achieved and worse estimations can be detected by low values of $\hat{\rho}$.

VIII. Conclusion and Further Work

This paper has presented two methods for estimating the pose of a mobile robot. The methods are based on a radio map and use RSS values of WLAN APs in range. In order to reduce the density of calibration points in the radio map, Delaunay triangulation and weigthed Euclidean distance is applied to interpolate the position of the mobile robot. Furthermore the estimation of the heading of a mobile robot with the aid of a beam antenna was presented. Since the accuracy of the

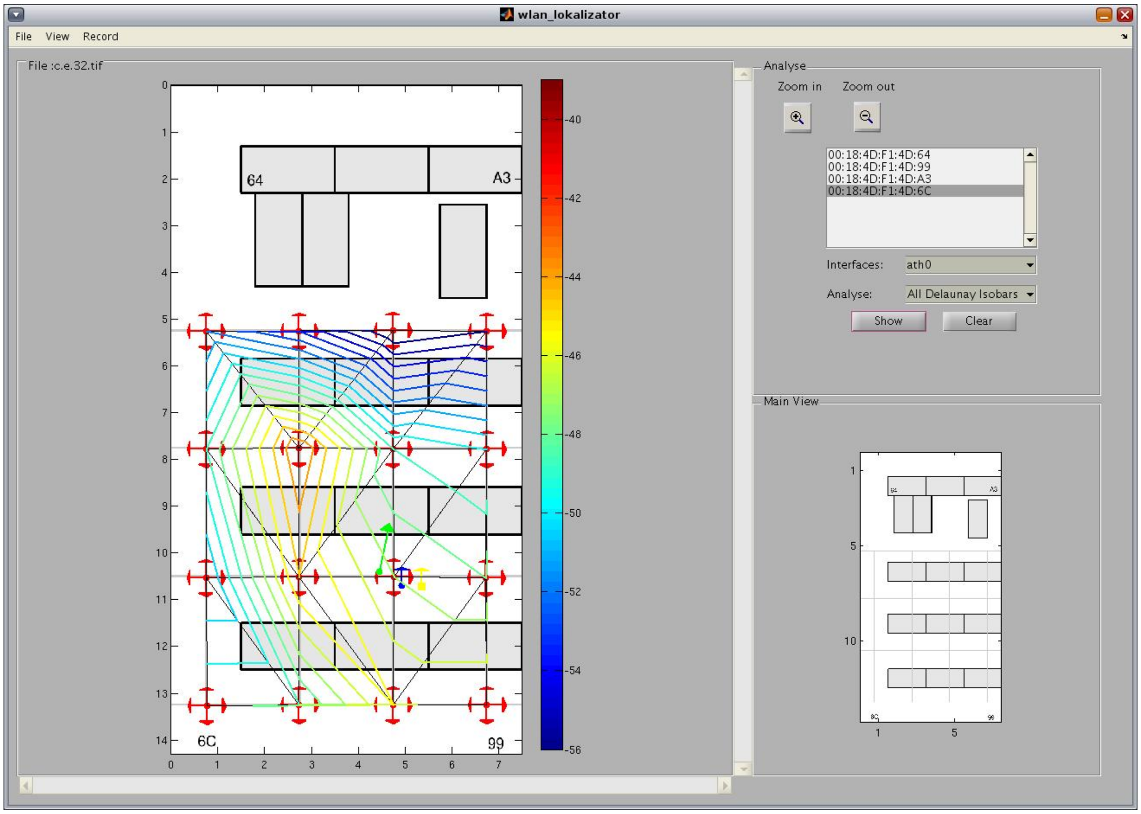

Fig. 13. Matlab Localization engine and GUI

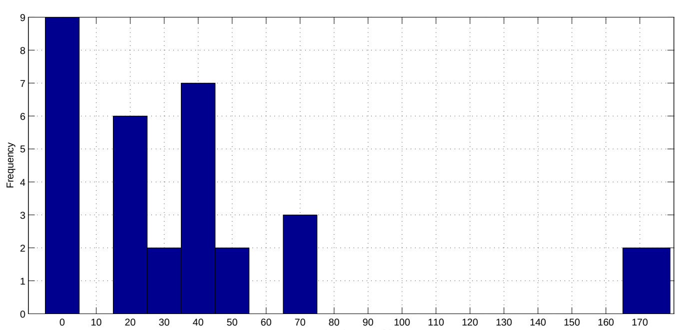

Fig. 16. Histogram of estimation error of heading

estimation depends highly on the positions of the APs in the environment, the placement of the APs has to be optimized, in order to get a good and reliable position estimation.

In future work the accuracy of the estimation should be improved by using a Kalman filter or a Monte Carlo particle filter. Furthermore the accuracy may be improved by fusion with position information obtained from other sensor e.g. odometry, sonar or laser.

References

[1] D. Fox, "KLD-Sampling: Adaptive Particle Filters and Mobile Robot Localization," University of Washington, Technical Report UW-CSE-01-08-02, 2002.

[2] S. Thrun, "Probabilistic Algorithms in Robotics," *AI Magazine*, vol. 21, no. 4, pp. 93–109, 2000.

[3] C. Röhrig and F. Künemund, "Estimation of Position and Orientation of Mobile Systems in a Wireless LAN," in *Proceedings of the 46th IEEE Conference on Decision and Control*, New Orleans, USA, Dec. 2007, pp. 4932–4937.

[4] A. Sayed, A. Tarighat, and N. Khajehnouri, "Network-based Wireless Location: Challenges faced in Developing Techniques for Accurate Wireless Location Information," *Signal Processing Magazine*, vol. 22, no. 4, pp. 24–40, July 2005.

[5] Guolin Sun, Jie Chen, Wei Guo, and K. Liu, "Signal Processing Techniques in Network-aided Positioning: A Survey of State-of-the-art Positioning Designs," *Signal Processing Magazine*, vol. 22, no. 4, pp. 12–23, July 2005.

[6] S. Feldmann, T. Hartmann, and K. Kyamakya, "An indoor Bluetooth-based Positioning System: Concept, Implementation and Experimental Evaluation," in *Proceedings of the International Conference on Wireless Networks*, Las Vegas, USA, June 2003, pp. 109–113.

[7] K. Michael and L. McCathie, "The Pros and Cons of RFID in Supply Chain Management," in *Proceedings of the International Conference on Mobile Business*, Sydney, Australia, July 2005, pp. 623–629.

[8] D. Hähnel, W. Burgard, D. Fox, K. Fishkin, and M. Philipose, "Mapping and Localization with RFID Technology," in *Proceedings of the International Conference on Robotics and Automation*, vol. 1, New Orleans, USA, May 2004, pp. 1015–1020.

[9] J. Koch, J. Wettach, and E. Bloch, "Indoor Localisation of Humans, Objects, and Mobile Robots with RFID Infrastructure," in *Proceedings of the 7th International Conference on Hybrid Intelligent Systems*, Kaiserslautern, Germany, Sept. 2007, pp. 271–276.

[10] A. Nasipuri and K. Li, "A Directionality based Location Discovery Scheme for Wireless Sensor Networks," in *Proceedings of the 1st ACM International Workshop on Wireless Sensor Networks and Applications*, Atlanta, USA, Sept. 2002, pp. 105–111.

[11] N. B. Priyantha, A. K. L. Miu, H. Balakrishnan, and S. Teller, "The Cricket Compass for Context-aware Mobile Applications," in *Proceedings of the 7th Annual International Conference on Mobile Computing and Networking*, Rome, Italy, July 2001, pp. 1–14.

[12] P. Alriksson and A. Rantzer, "Experimental Evaluation of a Distributed Kalman Filter Algorithm," in *Proceedings of the 46th IEEE Conference on Decision and Control*, New Orleans, Dec. 2007, pp. 5499–5504.

[13] N. Patwari, A. O. Hero, M. Perkins, N. S. Correal, and R. O'Dea, "Relative Location Estimation in Wireless Sensor Networks," *IEEE Transactions on Signal Processing*, vol. 51, no. 8, pp. 2137–2148, 2003.

[14] P. Bahl and V. N. Padmanabhan, "RADAR: An In-Building RF-based User Location and Tracking System," in *Proceedings of the 19th Annual Joint Conference of the IEEE Computer and Communications Societies*, vol. 2, Tel Aviv, Israel, Mar. 2000, pp. 775–784.

[15] A. M. Ladd, K. E. Bekris, A. Rudys, D. S. Wallach, and L. E. Kavraki, "On the Feasibility of Using Wireless Ethernet for Indoor Localization," *IEEE Transaction on Robotics and Automation*, vol. 20, no. 3, pp. 555–559, June 2004.

[16] U. Großmann, C. Röhrig, S. Hakobyan, T. Domin, and M. Dalhaus, "WLAN Indoor Positioning based on Euclidian Distance and Interpolation (Isobars)," in *Proceedings of the 8th Wireless Technologies Kongress*, Dortmund, Germany, 2006, pp. 296–305.

[17] R. Kumar K., V. Apte, and Y. A. Powar, "Improving the Accuracy of WLAN based Location Determination Using Kalman Filter and Multiple Observers," in *Proceedings of the Wireless Communications and Networking Conference*, vol. 1, Las Vegas, Apr. 2006, pp. 463–468.

[18] L. Hu and D. Evans, "Localization for Mobile Sensor Networks," in *Proceedings of the 10th Annual International Conference on Mobile Computing and Networking*, 2004, pp. 45–57.

[19] F. Moster and A. Tews, "Practical WiFi Localization for Autonomous Industrial Vehicles," in *Proceedings of the Australasian Conference on Robotics and Automation 2006*, Auckland, New Zealand, Dec. 2006.

[20] M. Brunato and R. Battiti, "Statistical Learning Theory for Location Fingerprinting in Wireless LANs," *Computer Networks*, vol. 47, no. 6, pp. 825–845, Apr. 2005.

[21] J. J. Astrain, J. Villadangos, J. Garitagoitia, J. González de Mendívil, and V. Cholvi, "Fuzzy Location and Tracking on Wireless Networks," in *Proceedings of 4th ACM International Workshop on Mobility Management and Wireless Access*, Torremolinos, Spain, Oct. 2006, pp. 84–91.

[22] A. Teuber and B. Eissfeller, "WLAN Indoor Positioning Based on Euclidean Distances and Fuzzy Logic," in *Proceedings of the 3rd Workshop on Positioning, Navigation and Communication*, 2006, pp. 159–168.

[23] M. Ocana, L. Bergasa, M. Sotelo, J. Nuevo, and R. Flores, "Indoor Robot Localization System Using WiFi Signal Measure and Minimizing Calibration Effort," in *Proceedings of the IEEE International Symposium on Industrial Electronics*, vol. 4, 2005, pp. 1545–1550.

[24] G. Leach, "Improving Worst-Case Optimal Delaunay Triangulation Algorithms," in *Proceedings of the 4th Canadian Conference on Computational Geometry*, 1992.

[25] G. Anousaki and K. Kyriakopoulos, "Simultaneous Localization and Map Building of Skid-Steered Robots," *IEEE Robotics & Automation Magazine*, pp. 79–89, Mar. 2007.

[26] Activmedia, *Advanced Robotics Interface for Applications (ARIA) Developer's Reference Manual*, ActivMedia Robotics, 2006, http://robots.activmedia.com/ARIA.

[27] J. Tourrilhes, "Wireless Tools for Linux," http://www.hpl.hp.com/personal/Jean_Tourrilhes/Linux/Tools.html.

[28] A. M. Ladd, K. E. Bekris, A. Rudys, L. E. Kavraki, and D. S. Wallach, "Robotics-based Location Sensing Using Wireless Ethernet," *Wireless Networks*, vol. 11, no. 1-2, pp. 189–204, 2005.

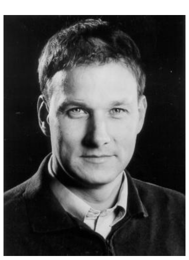

Christof Röhrig received his Diploma degree from the University of Bochum, Germany, in 1993, and his Doctor degree from the University of Hagen, Germany, in 2003, both in electrical engineering. Between 1993 and 1997 he was Manager Automated Systems Engineering at Reinoldus Transport- und Robotertechnik GmbH Dortmund, Germany. From 1997 until 2003 he was with the Control Systems Engineering Group at University of Hagen. His research was focused on motor control, eLearning and remote laboratories. Since 2003, he is Professor of Computer Science at the University of Applied Sciences Dortmund, Germany. His current research interests include robotics, mobile computing and telematics.

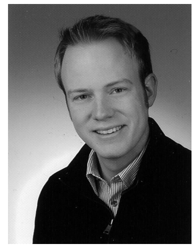

Frank Künemund received his Diploma degree from the University of Applied Sciences Dortmund, Germany, in 2008, in computer science. After his degree he works in the scientific staff of the University of Applied Sciences Dortmund. Furthermore he is a student of master of computer science degree course of the University of Applied Sciences Dortmund. His current research interests include robotics, localization and WLAN technologies .